

Urbanization signatures on climate and soils uncovered by crowd-sensed plants

Received: 26 May 2025

Accepted: 5 December 2025

Published online: 15 January 2026

 Check for updates

Susanne Tautenhahn¹✉, Martin Jung², Michael Rzanny¹, Patrick Mäder^{3,4,5}, Markus Reichstein², Bernhard Ahrens^{2,12}, Anke Bebber^{1,12}, David Boho^{3,12}, Milan Chytrý^{6,12}, Jürgen Dengler^{7,8,12}, Florian Jansen^{9,12}, Negin Katal^{2,11,12}, Gabriele Midolo^{10,12}, Lubomír Tichý^{6,12}, Sophia Walther^{2,12}, Ulrich Weber^{2,12}, Hans Christian Wittich^{3,12} & Jana Wäldchen^{1,5}

Human populations are increasingly concentrated in cities, creating some of Earth's most modified ecosystems. However, we lack concepts for assessing heterogeneous urban environments, especially their soils, at large spatial scales. Here we uncover fine-scale urban climate and soil patterns across 326 European cities by using more than 80 million crowd-sensed plant observations as living sensors of the environment. In addition to the urban heat island, we identify similar contrasts between the built-up and green areas for moisture, soil pH, salinity and soil disturbance. These within-city environmental contrasts correspond to differences between cities that are about 1,500–3,000 km apart. Climate, especially soil, conditions are more similar between cities for built-up areas than for forests, indicating urban homogenization tendencies. Urban forests serve as a source of environmental diversity, cooling and moisture retention. The crowd sensing of urban environments is facilitated by their citizens, which can support science, policy and help guide urban planning toward livable cities.

By 2050, nearly 70% of the global human population is predicted to live in urban areas¹. Urbanization alters environmental conditions and processes, as exemplified by the urban heat island phenomenon². This threatens important ecosystem services³ and increases the vulnerability of both ecosystems and humans to climate change¹. Urban planning must address these challenges to support multiple United Nations Sustainable Development Goals, including Sustainable Cities and Communities, Good Health and Well-being, Life on Land, and

Climate Action⁴. This is a complicated task, given that surprisingly little is known about how urbanization transforms physical environments in particular.

The urban heat island phenomenon stands out as the most intensively investigated and best understood consequence of urbanization on the environment^{2,5,6}, partly because it is relatively easy to measure in situ and by remote sensing. This facilitated recommendations to mitigate urban heat, such as the expansion of green spaces as a

¹Independent Research Group Biodiversity, Ecosystems, and Society, Max Planck Institute for Biogeochemistry, Jena, Germany. ²Department Biogeochemical Integration, Max Planck Institute for Biogeochemistry, Jena, Germany. ³Data-Intensive Systems and Visualisation, Technische Universität Ilmenau, Ilmenau, Germany. ⁴Faculty of Biological Sciences, Friedrich Schiller University Jena, Jena, Germany. ⁵German Centre for Integrative Biodiversity Research (iDiv), Halle-Jena-Leipzig, Leipzig, Germany. ⁶Department of Botany and Zoology, Faculty of Science, Masaryk University, Brno, Czech Republic. ⁷Vegetation Ecology Research Group, Institute of Natural Resource Sciences, Zurich University of Applied Sciences (ZHAW), Wädenswil, Switzerland. ⁸Bayreuth Center of Ecology and Environmental Research (BayCEER), University of Bayreuth, Bayreuth, Germany. ⁹Faculty of Agriculture, Civil and Environmental Engineering, University of Rostock, Rostock, Germany. ¹⁰Department of Spatial Sciences, Faculty of Environmental Sciences, Czech University of Life Sciences Prague, Praha-Suchbát, Czech Republic. ¹¹Present address: Faculty of Environment and Natural Resources, Chair of Sensor-based Geoinformatics, University of Freiburg, Freiburg, Germany. ¹²These authors contributed equally: Bernhard Ahrens, Anke Bebber, David Boho, Milan Chytrý, Jürgen Dengler, Florian Jansen, Negin Katal, Gabriele Midolo, Lubomír Tichý, Sophia Walther, Ulrich Weber, Hans Christian Wittich.

✉e-mail: staut@bgc-jena.mpg.de

nature-based solution^{7,8}. However, other consequences of urbanization on the environment and, hence, ecosystem services are largely unknown or uncertain, and it is unclear whether these consequences extend to generalized phenomena. Case studies showed reduced relative humidity over cities^{9,10} and postulated an urban dry island pattern. By contrast, a global meta-analysis suggests increased precipitation over urban areas on average, but highlights large variability¹¹. However, in particular, soils—key regulators of ecosystem services and functions—remain to be a blind spot in general^{12,13}. Studies reflect heterogeneous patterns of urban soil compaction, sealing, disturbance, pollution, and frequent soil replacement or mixing through construction and landscaping^{14–16}. A tendency toward an increased soil pH and reduced fertility was found and attributed to vehicle exhaust and calcium in construction materials^{17–19}.

Given the heterogeneity and complexity of urbanization impacts on the environment, it seems questionable whether generalized patterns extend beyond the urban heat island phenomenon at all. However, the establishment of urban residential, commercial, industrial and green spaces tends to follow repetitive and similar patterns between cities, which could lead to an anthropogenic urban structure with uniform environmental characteristics. This rationale entails the paradigm of ‘urban homogenization’, which has been supported by remotely sensed evidence on the urban form (that is, their spatial composition and compactness), and heat island patterns^{20,21} as well as for plant and bird communities^{22,23}. A case study from six US cities found that humidity conditions and soil organic carbon stocks in residential areas were indeed more similar between cities than between their natural surroundings²⁴. However, the extent to which urban homogenization applies to climate and soil conditions remains unclear.

Our critical knowledge gaps on urban climate and soils result from the lack of observational concepts that are adequate for the heterogeneous nature of cities, and which are applicable over continental to global scales. Extensive, detailed in situ monitoring networks for urban environments seem infeasible, and remote sensing, being indispensable, can only inform about few environmental variables directly. However, millions of citizens experience their environment every day. This collective experience presents a novel opportunity to sense urban environments by leveraging the popularity of artificial-intelligence-based plant identification apps and the principle of bioindication—the ability to infer environmental conditions indirectly from species’ occurrences based on their ecological requirements^{25,26}.

Here we capitalize on more than 80 million crowd-sensed observations of over 15,000 plant species for which ecological indicator values are available, allowing their use as living sensors, to map climatic and soil conditions in 326 European cities. We generate high-resolution (~100 m) maps of bioindicated temperature, moisture, light, soil pH, fertility, salinity and disturbance, and analyze how these vary by urban land-use type within and between cities. We show that urban land-use environments across Europe feature systematic variations of not only temperature but also moisture, light and soil properties with urban climates and soils, which are locally diverse and homogenized across cities at the same time.

Uncovering urban environments by crowd-sensed plant observations

We combine crowd-sensed plant occurrence data with recently developed quantitative indicator value systems for European plants^{27–29} to map climate and soil conditions (Table 1)—we call this approach mobile crowd sensing of environments (MCSE) (Fig. 1 and Methods). Plant’s ecological indicator values associate plant species with scores describing their typical occurrence along an environmental gradient (for example, temperature or soil pH), based on botanical expertise acquired over decades^{26,30}. By combining the presence of co-occurring species and their indicator scores, a robust picture of the environmental

Table 1 | Interpretation of environmental factors derived from bioindication of climate and soil conditions used in this study

Environmental factor	Interpretation
Climate	
Temperature ^{27,28}	Bioclimatic temperature, highly correlated with mean annual temperature and mean temperature of the warmest quarter ²⁷
Light ^{27,28}	Local light conditions affected by canopy cover or shading ²⁶
Moisture ^{27,28}	Local moisture conditions related to vapour pressure deficit ²⁶ , soil moisture content and tension ^{26,28}
Soil	
Nutrients ^{27,28}	Overall fertility for biomass production, reflecting different plant-available nutrients, only weakly correlated with nitrogen mineralization and available mineral nitrogen ^{26,28}
Salinity ²⁸	Abundance of salts such as sodium chloride, magnesium sulfate, sodium sulfate, calcium sulfate or sodium carbonate
Reaction ^{27,28}	Soil’s acidity or alkalinity for example due to variations in calcium ²⁶ , linearly or curvilinearly related to soil pH ²⁶
Disturbance ²⁹	Amount of bare ground cover caused by furrowing or soil turning ²⁹

variable of interest can be obtained locally²⁶. However, limited species distribution data had restricted the applicability of this concept.

Since hundreds of thousands of people participate in capturing plant occurrences with species identification apps across urban areas, the increasing availability of such opportunistic crowd-sensed data unlocks the potential to map environmental conditions for unprecedented spatial extents and resolutions. For each environmental variable listed in Table 1, we calculate the mean indicator value of all species recorded in a 0.00166° grid cell (~100 m) (Fig. 1d–f and Extended Data Fig. 1a–d), irrespective of the number of occurrences per species, for 326 European cities ranging from Southern to Nordic countries. We also produce maps for Europe at a spatial resolution of 0.1666° (~10 km) (Fig. 1d–f and Extended Data Fig. 1a–d) for evaluation and illustration of the approach since independent in situ data for validation from cities are scarce.

Variations in temperature, soil reaction, soil disturbance, light, soil moisture, soil nutrients and salinity across Europe derived by MCSE (Fig. 1d–f and Extended Data Fig. 1) show spatially coherent patterns that are consistent with expected environmental variation and independent data (Extended Data Fig. 2). For example, the gradual temperature changes from the warm Mediterranean to the cool boreal region are clearly evident along with elevational modulations by mountain ranges such as the Alps, Pyrenees and Scandes. The low soil reaction (soil pH) in the Scandes is due to the geological prevalence of acidic rocks in conjunction with the acidity of the coniferous needle litter of boreal forests. Mountain ranges are associated with low soil disturbance compared with most of Europe under more intense management and land use. Even at the scale of individual cities, we can observe spatially coherent patterns (Fig. 1c), such as cooler temperatures in the vegetated floodplain of the river Isar, and the highest temperatures in the city center of Munich. In Hanover, the lowest soil disturbance is associated with urban forests, whereas intensive agricultural use at the city fringes shows the largest signs of soil disturbance. We emphasize that the spatially coherent patterns of MCSE originate merely from crowd-sensed plant observations without any additional aid from other spatial data sources. This implies a robustness of the opportunistic MCSE approach against various sampling biases (for example, potential misidentifications or biases toward beautiful, flowering plants, in

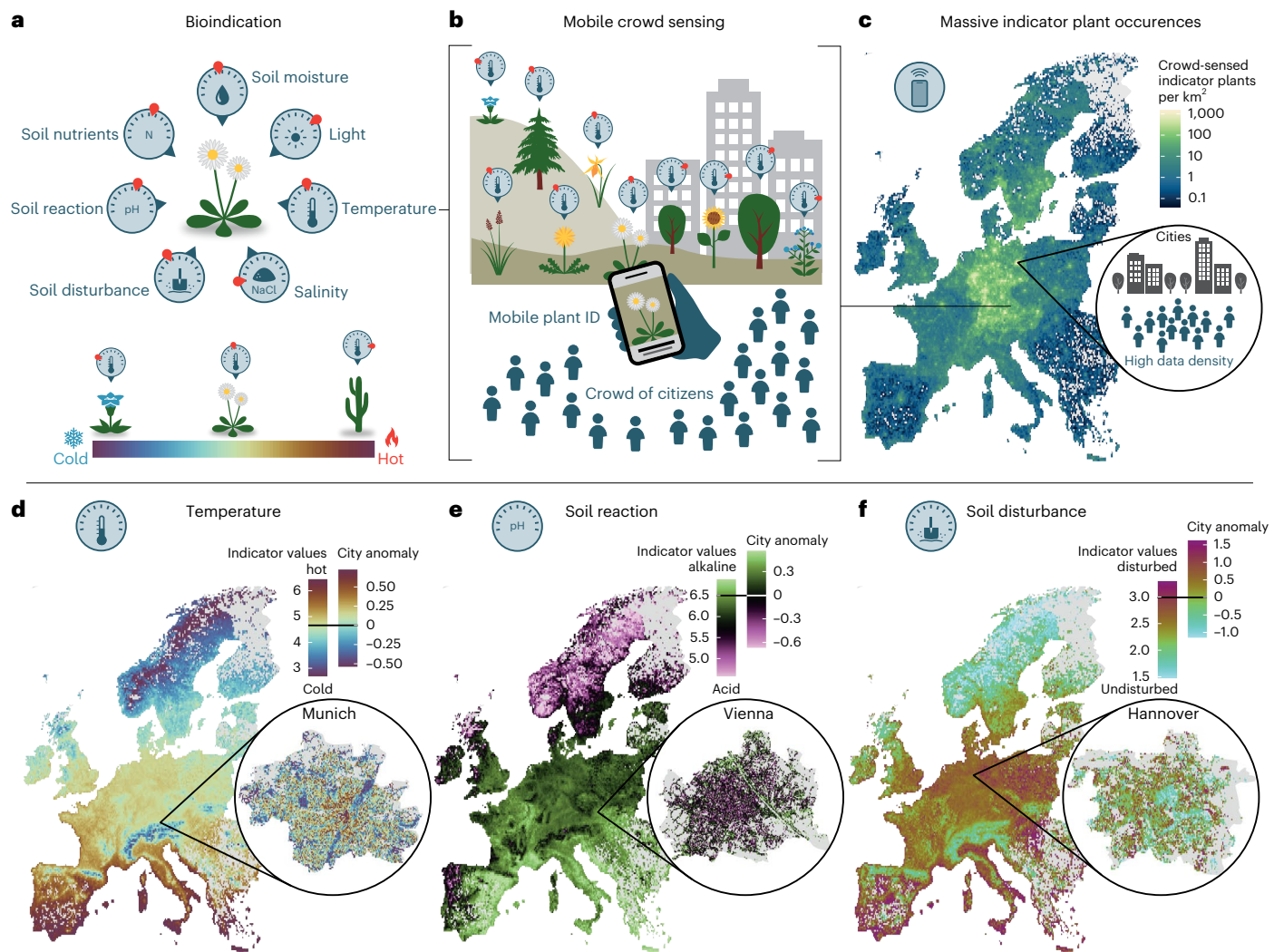


Fig. 1 | Concept of MCSE. a, Bioindication assigns species-specific indicator values for climate (temperature, light and moisture) and soil (nutrients, salinity, reaction and disturbance) conditions. Environmental gradients are reflected by a changing mean indicator value of the occurring species, illustrated for temperature. **b**, Mobile crowd sensing utilizes extensive acquisitions of species occurrences by citizens using automated plant identification apps for smartphones. Combined with the bioindication principle, spatial environmental gradients can be uncovered, for example, for temperature showing warmer

conditions in cities compared with nearby mountain ranges. **c**, Large amounts of indicator plant occurrences are accumulating rapidly over large spatial domains, such as Europe. **d–f**, This allowed for mapping environmental conditions across Europe at a spatial resolution of 0.166° (~10 km), and at much finer resolution (0.00166°, ~100 m) for cities due to higher observation densities. Please note that the color scales for Europe (left) and cities (right) differ. Extended Data Fig. 1 shows complementary figures for light, moisture, nutrients and salinity.

region or season). This is further corroborated by assessments against 40,000 expert-based vegetation surveys (Extended Data Fig. 3), and by an overall robustness against variations in data quality criteria for the crowd-sensed plant occurrence data (Extended Data Fig. 4).

Land-use signatures of climate and soil variables beyond the urban heat island

We analyzed how environmental conditions of 326 cities vary with urban land-use types in five regions of Europe (Nordic, Eastern, British Isles, Central and Southern) (Extended Data Fig. 5 and Methods). The city domains are based on municipalities, which typically include peri-urban areas with higher shares of forest, and agricultural areas besides built-up urban fabric (industrial and commercial units, continuous and discontinuous urban fabric) interspersed with green urban spaces. For each city, the mean indicator value across land-use types serves as a baseline—the variations of these ‘city means’ among regions (Fig. 2a) reflect expected large-scale gradients in Europe, as noted above (Fig. 1b and Extended Data Fig. 1).

Temperature anomalies associated with urban land use (that is, the mean land-use specific deviations from the city mean; Fig. 2b) reflect the well-known urban heat island phenomenon², with the largest temperatures for built-up areas and smallest for forests. This finding is consistent with many previous studies showing the strongest urban heat in the city centers with continuous urban fabric^{5,6}, and a relative cooling effect for vegetated land uses, especially forests³¹. Although the temperature anomaly patterns are overall consistent between regions, the additional heat of continuous urban fabric is less pronounced in cities of southern countries. This can be explained by a smaller contrast of surface properties between densely built-up areas and the naturally sparsely vegetated Mediterranean compared with wetter regions. This interpretation is supported by an attenuated contrast of the light indicator between forest and built up of cities from southern countries (Extended Data Figs. 6 and 7), because the indicated light conditions are strongly affected by shading due to tree canopies²⁶. Although the light anomalies with urban land use also show patterns that are consistent among regions, they show notable differences to the temperature

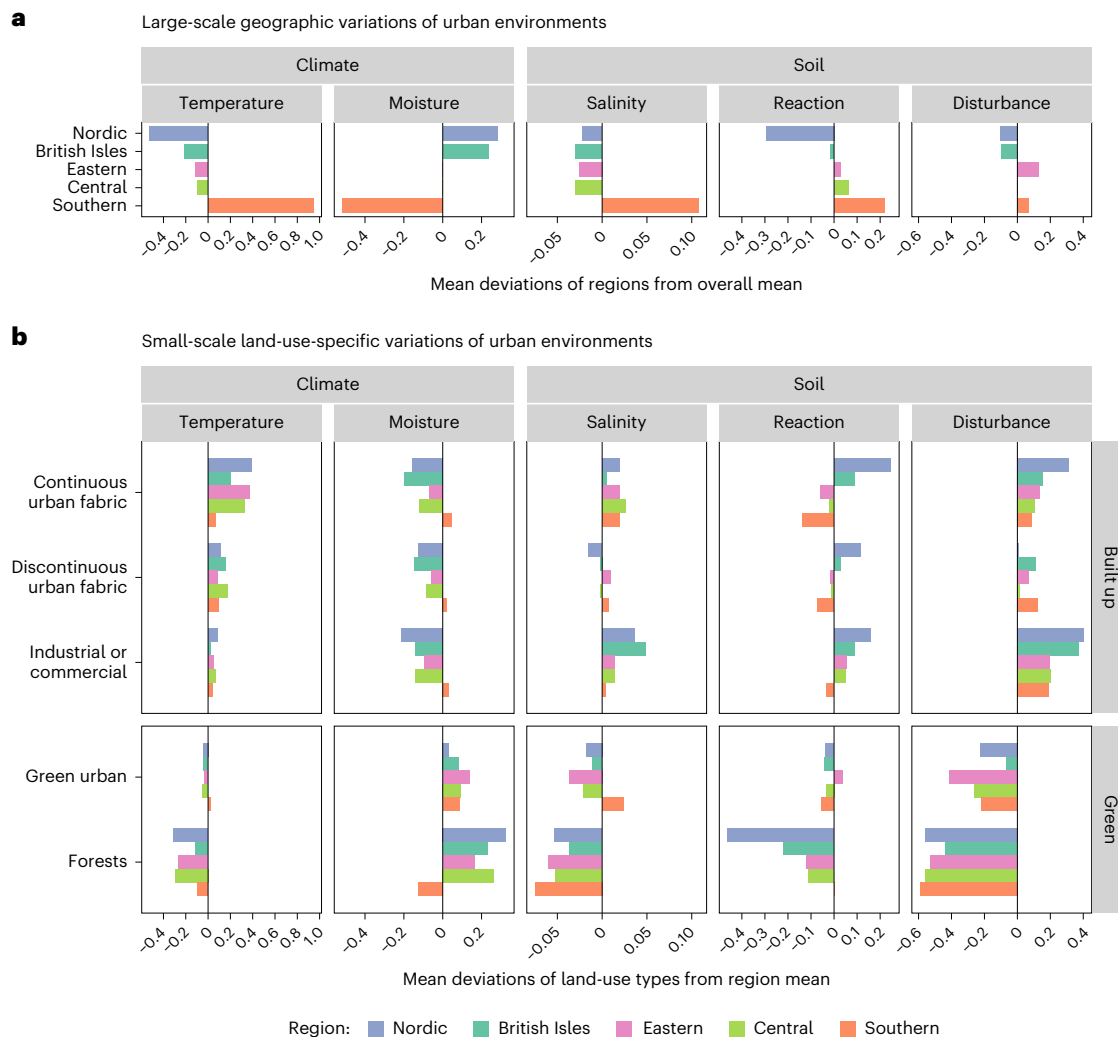


Fig. 2 | Urban environmental variation of European cities inferred by MCSE.

a, Between-region variations of city-mean conditions plotted as region deviations from the overall mean. For example, the climatic gradients ranging from the warm and dry Southern countries to the cool and moist Nordic countries are shown. **b**, Within-city variations by urban land use are plotted as mean deviations of land-use types from the region mean. Besides the well-known urban heat island phenomenon, parallel patterns of consistent environmental land-use profiles across regions are also evident for moisture, soil disturbance and salinity. Panels **a** and **b** show a consistent scale for comparison of the environmental gradients between regions and between land-use types within

cities. Results are based on the marginal effects obtained by a mixed-effect analysis of variance (fixed effects: region, land-use class and their interaction; random intercept: city) for each environmental variable of 326 cities (Nordic ($n = 19$), Eastern ($n = 31$), Central ($n = 188$), British Isles ($n = 45$) and Southern ($n = 31$); Methods). Extended Data Fig. 6 shows the results including light, soil nutrients and agricultural land use and Extended Data Fig. 7 shows the results based on biogeographic regions instead of planning families. Estimated marginal means, standard errors and 95% confidence intervals of model parameters are provided in the.

patterns, indicating the complex interplay of factors causing the urban heat island phenomenon^{5,6}.

Built-up land use is also drier than green urban (and agricultural land uses; Extended Data Figs. 6 and 7), with forests showing the largest positive moisture anomalies. This general pattern of an urban dry island is qualitatively consistent with reduced atmospheric dryness, as shown in previous studies^{9,32,33}. The dryness was primarily attributed to reduced evaporation, associated with the sealed urban built up, as well as higher temperatures³⁴. However, there are notable deviations in the Southern region: forests, and to a lesser extent, pastures (Extended Data Figs. 6 and 7), are drier, whereas built-up areas and especially urban green areas are wetter. This pattern probably reflects irrigation practices in Mediterranean cities, which increase inner-city moisture levels, whereas more natural vegetation such as forests and pastures often occurs on rocky terrains that are characteristically dry.

Soil disturbance shows consistent patterns across regions, with the largest values for built-up areas and arable land (Extended Data

Figs. 6 and 7), whereas forests and green urban areas are less affected. Interestingly, the salinity anomalies behave similarly, which may reflect increased pollution associated with anthropogenic impacts on urban soils, for example, salt application for deicing. Soil reaction, especially nutrients (Extended Data Figs. 6 and 7), show overall weaker associations with urban land use and weaker consistency between regions, whereas some individual patterns emerge. For example, Nordic soils of continuous urban fabric are relatively more fertile and alkaline than in other regions, which indicates that these soils were manipulated or exchanged to counteract the prevalent nutrient-poor and acidic soils in this region (Fig. 2a). This interpretation is supported by the large positive anomaly for soil disturbance of Nordic soils in continuous urban fabric. The soil pH is the lowest in forests compared with all other land-use types. This may be attributed to cation leaching with increased moisture³⁵, and to a greater abundance of organic acids, especially in the Nordic forests where conifers dominate. Soils in urban built up tend to be more alkaline than in forests, and previous hypotheses suggest

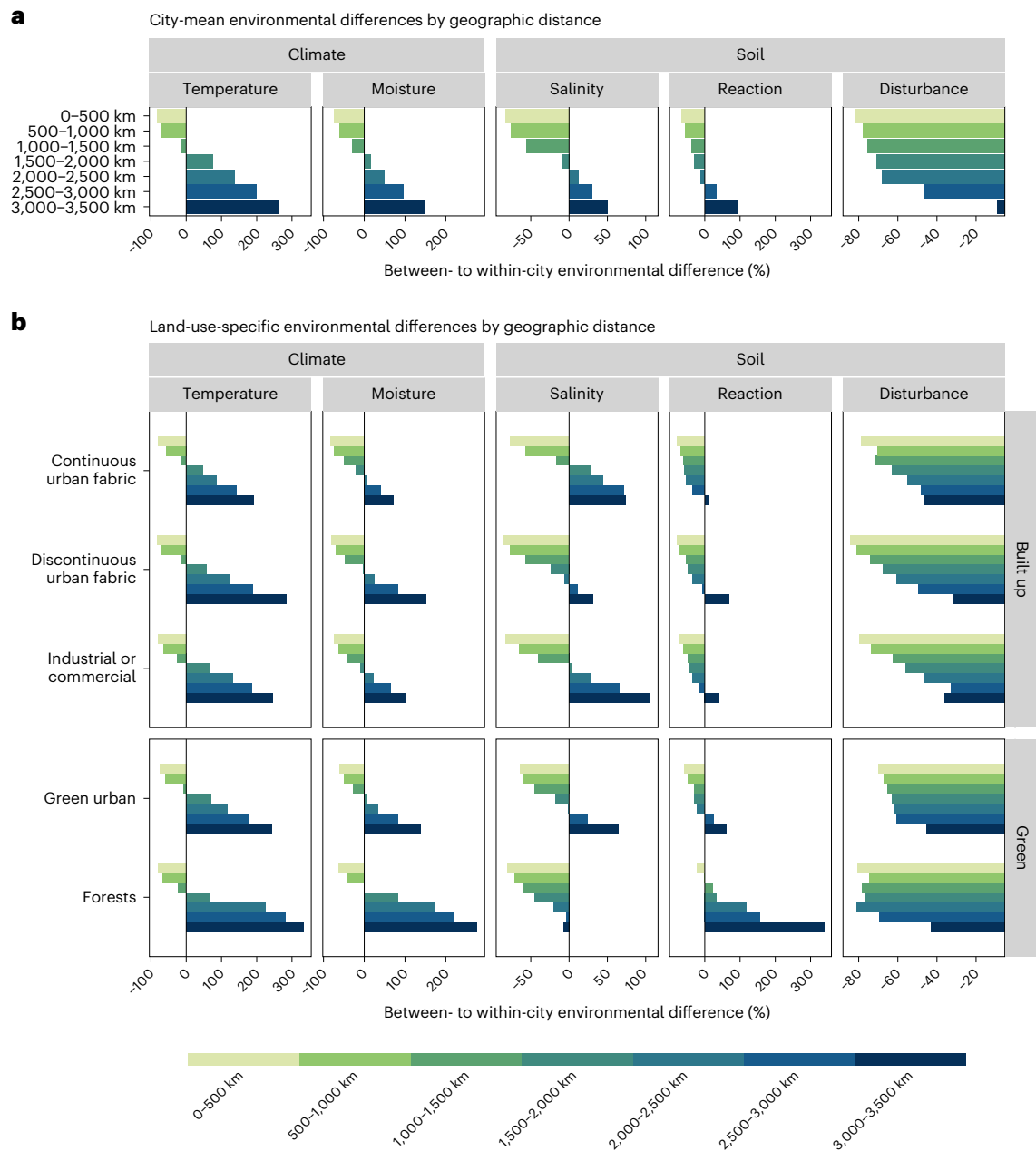


Fig. 3 | Between- to within-city environmental differences. Relative differences of median values stratified by geographic distances between cities are plotted (Methods). Negative values indicate within-city environmental differences to be larger than between-city environmental differences. **a**, Relative differences for city-mean environmental conditions show that within-city variations among land-use types exceed differences between cities up to 2,000 km apart (negative values) for all the considered environmental factors. **b**, Environmental

differences between cities by land-use type show that these are generally larger for forests than others, especially built up, land-use types, which is most evident when comparing cities that are more than 2,000 km apart. Extended Data Fig. 8 shows the results including light, soil nutrients and agricultural land use. Relative and absolute differences as well as the corresponding standard deviations are provided in the.

a relationship with calcium abundance originating from construction materials, vehicle exhaust or deicing^{17,36}. However, this may not explain our finding of elevated soil pH of arable land and pastures (Extended Data Figs. 6 and 7).

Overall, we uncovered variations in climate and soil factors by urban land-use type that are largely consistent between regions in Europe. These extend beyond the urban heat island phenomenon, presenting comparable patterns for light, moisture, soil disturbance, salinity and, to a lesser extent, for soil pH—all forming a gradient from urban forests at one end to heavily modified build-up land-use types at the other end. Strikingly, the range of environmental

conditions between urban land-use types is of comparable magnitude to the range of environmental conditions between regions (compare Fig. 2a,b). This indicates a substantial environmental diversity within cities compared with variations between cities, ranging from Southern to Nordic countries.

Locally diverse urban climates and soils are homogenized across cities

To contextualize urban environmental gradients, we compare environmental differences within a city, associated with land use, to those between cities, stratified by spatial distances of 500 km (Methods).

For interpretation: a relative difference of 50% would mean that the environmental differences between cities are 50% larger than the environmental gradient within a city. As expected, environmental differences between cities increase with geographical distance (Fig. 3a), a pattern known as the ‘distance decay of similarity’, once coined as the ‘first law of geography’^{37,38}. However, we find that within-city gradients exceed differences between cities up to about 1,500 km apart (that is, negative relative differences are shown in Fig. 3a) for climate variables, whereas for soil factors, this threshold extends beyond 2,000 km. For example, the temperature gradients between urban land-use types within cities are comparable with the temperature gradient of about 1,500 km in Europe. For soil pH, salinity and light (Extended Data Fig. 8), this holds even for geographic distances of >2,000 km, whereas for soil disturbance and nutrients within-city difference dominate over the full range of considered distances up to 1,500 km. This is partly because these factors can also vary strongly at smaller scales. Nevertheless, this illustrates the large environmental gradients within cities associated by diverse urban land-use types relative to large-scale, nearly continental variations. Even though cities were often established in areas with high geodiversity to capitalize on various ecosystem services³⁹, urbanization has most probably increased environmental gradients locally, causing contrasts to more natural areas like forests across much of Europe. But can we reconcile the observed local diversity of urban environments with the paradigm of urban homogenization, which postulates convergence among cities as they adopt similar land-use practices and urban planning?

To understand to what extent urban environments were homogenized among cities, we compare the relative environmental gradients per land-use type, and assess the difference between anthropogenic built-up land use to the more natural ones, like forests (Fig. 3b). We find that the environmental similarity between cities decays less with spatial distance in urban built-up areas than in urban forests. The contrast between urban built-up areas and forests is particularly large for soil pH and light but it also holds true for moisture and temperature (Extended Data Fig. 8). Interestingly, soil salinity and disturbance, both indicating anthropogenically deteriorated soils, behave differently, which points to regional differences in urban planning, implementation and management. Otherwise, forests are less influenced by human activities and show greater environmental diversity between cities. By contrast, built-up areas, shaped to meet the narrow range of human needs, tend to be more similar across different cities. Thus, urbanization tends to reduce the environmental variability between cities, supporting the hypothesis of urban environmental homogenization in Europe. This is qualitatively consistent with a study from six metropolitan areas in the US²⁴, and helps to explain evidence for the homogenization of urban biota²², including the soil microbiome⁴⁰. Urbanization in Europe appears to foster homogenization among cities and creating local diversity at the same time.

Conclusions and implications

We revealed distinct common land-use patterns of climate and soil conditions in urban Europe, which are indicative of anthropogenic imprints on the environment. These environmental variations by urban land-use type go beyond the well-known urban heat island effect, with comparable patterns observed for light, moisture, soil disturbance, salinity, and, to a lesser extent, soil reaction. Built-up areas are not only warmer but also drier, brighter, more disturbed, more alkaline and polluted by salt than urban green spaces, especially forests. These alterations translate into large environmental gradients within cities that are comparable with—or even greater than—those observed between cities more than 1,500 to 3,000 km apart. Although urbanization seems to promote large environmental diversity within cities, the repeated establishment of similar urban built-up fabric leads to the homogenization of soil and climate conditions across European cities. These findings reconcile the

paradigm of urban homogenization with patterns of substantial local but limited large-scale diversity for climate and soil factors.

Fundamentally, urbanization involves fast growing residential, commercial and industrial built-up areas threatening or replacing green spaces such as forests^{41–43}. The resulting loss of environmental diversity and ecosystem functions degrades essential ecosystem services like cooling, moisture retention and soil multifunctionality, with cascading effects on biodiversity^{44,45}, human health^{41,46} and well-being^{47,48}. Our results emphasize that conserving and creating multifunctional urban green spaces, especially forests, is a nature-based solution to enhance urban resilience by mitigating the negative impacts of urbanization and climate change. Environmental assessments by mobile crowd sensing offer unprecedented cost- and time-effective opportunities for science and decision-makers to guide locally tailored, sustainable urban planning. Leveraging the rapidly growing citizen participation can facilitate fine-grained environmental monitoring of rapidly evolving urban socioecosystems and, therefore, contribute to livable cities and to achieve Sustainable Development Goals.

Methods

MCSE

We compiled crowd-sensed plant occurrence data of Europe, collected from several citizen science initiatives: the plant identification apps Flora Incognita⁴⁹ and Pl@ntNet^{50,51}, as well as species-reporting platforms such as iNaturalist⁵², Observation.org⁵³, Naturgucker.de⁵⁴, Artportalen⁵⁵, the Norwegian species observation service⁵⁶, INPN⁵⁷, Arter.dk⁵⁸, FinBIF⁵⁹ and iRecord^{60,61}. Except for Flora Incognita, all other data were downloaded from the Global Biodiversity Information Facility (GBIF) using the `rgbif` package⁶². We applied the following filter criteria: “no geospatial issues”; “coordinates available”; “coordinate uncertainty less than 500 m”; “basis of record: human observation, observation, or machine observation”; “occurrence status: present”; and “recorded between 2000 and 2024”.

We merged the crowd-sensed plant occurrence data with ecological indicator values of climate and soil conditions (Table 1), which are specific to vascular plant taxa (aggregates, species and subspecies), and available from three pan-European systems^{27–29}. To resolve differences in species-naming conventions in the plant occurrence data and the indicator value systems used, we standardized all species names using the GBIF backbone taxonomy and the `rgbif` package⁶². This intersection yielded 81,410,220 crowd-sensed observations of 15,413 taxa in Europe, which we used to generate maps of climate and soil variables across Europe and for European cities. The indicator for soil disturbance was calculated based on ref. 29; for salt, based on ref. 28; and the remaining, based on ref. 27. To ensure that indicator values are comparable across the three indicator value systems used^{27–29}, we rescaled all systems to a common range of 0 to 10. Please note that 0 and 10 are theoretical bounds, which are not realized in practice due to the co-occurrence of different species with different indicator values assigned.

We generated maps of MCSE-based climate and soil conditions for Europe with a spatial resolution of 10 arcmin (0.166°, ~10 km) for illustration (Fig. 1) and evaluation purposes. The European domain is defined by the CORINE land cover data product⁶³, which excludes parts of eastern Europe. We also exclude Türkiye because indicator value systems are not applicable there^{27–29}. For each grid-cell and environmental factor, we calculated the mean indicator value of at least 25 different species observed in the grid cell—if less than 25 species were available, a missing value was assigned. This setting was derived from extensive sensitivity tests for maximizing data coverage and maintaining high accuracy. This analysis involved further assessments with respect to applying a threshold for the minimum number of observations per species, and the consideration of weighing species by observation frequency (abundance) instead of presence/absence (see below for details).

The high data availability of plant occurrence data in urban areas allowed us to map climate and soil factors for European cities at a much finer spatial resolution of 0.1 arcmin (0.0016°, ~100 m). The city domains are municipalities available as polygon information by Eurostat European Urban audit (<https://ec.europa.eu/eurostat/web/regions-and-cities>), restricted to cities with more than 50,000 inhabitants and downloaded with R package *giscoR*⁶⁴. We mapped mean climate and soil indicator values using a threshold of a minimum of five different indicator species per grid cell. We kept 326 European cities for final analysis, which satisfied urban land-use specific data coverage criteria (see below).

Sensitivity analysis and evaluation with independent data

We used independent datasets for the mean annual temperature of WORLDCLIM⁶⁵ and the pH of the topsoil (0–5-cm depth) predicted by SoilGrids⁶⁶ in Europe to evaluate the temperature and soil reaction based on MCSE. These datasets were resampled to match the 0.166° resolution of MCSE for Europe and used to calculate the Spearman's rank correlation coefficient with the corresponding data from MCSE. The corroboration (Extended Data Fig. 2) shows an excellent agreement ($r = 0.96$) and linear relationship for temperature. The relationship with soil pH is also linear above a pH value of 5, whereas an apparent saturation of the SoilGrids product around a value of 4.5 deteriorates the correlation to 0.86. A similar saturation effect was found for mapping soil pH in Switzerland based on random forests⁶⁷, which is the same method used for generating SoilGrids. Thus, a direct validation is hampered by uncertainties of the SoilGrids product that may be caused by the sparsity of in situ observations and the challenges of extrapolation, as well as issues of capturing the spatial heterogeneity of soil conditions. These findings are consistent with previous case studies on smaller scales in which the bioindication approach even outperformed traditional environmental data products^{68–71}, and underscore the potential of using plants as living sensors of the environment in an urban context⁷².

We used the rank correlation coefficient of MCSE products with WORLDCLIM and SoilGrids as a metric to assess the robustness against methodological choices, as well as to derive settings that achieve a high spatial coverage of MCSE, maintaining high correlations. We executed a comprehensive full-factorial sensitivity analysis by varying the following settings: (1) indicator system used (ref. 27 versus ref. 28); (2) computation of mean values based on presence-only data of species occurrences versus weighing species by observation frequencies; (3) the threshold of the minimum number of required indicator species per grid cell as a measure of completeness in the crowd sensing of plants; and (4) the minimum number of observations per indicator species as a reliability measure of species occurrence. The respective results (Extended Data Fig. 4) indicate (1) minor differences among indicator systems; (2) a systematic preference for presence only over observation-frequency-weighted data treatment; and (3) a high overall robustness of the correlation against different filter choices for the minimum number of required species and observations per species (see the range of the color bar in Extended Data Fig. 4). Therefore, we chose the presence approach, and put no threshold on the minimum number of observations per species to maximize spatial coverage. Our results from the sensitivity analysis are qualitatively consistent with a case study in Switzerland using expert-based vegetation plots⁷³.

To further assess the potential biases in plant occurrences captured by citizen scientists—such as misidentifications, preferences of visually appealing plants, biases in certain season or regions—we compared the quality of MCSE with bioindication based on expert vegetation data. Therefore, we calculated the mean indicator values (based on presence only) of temperature and soil pH for 40,000 vegetation plots (*sPlotOpen*⁷⁴) in which the abovementioned biases should not occur, and correlated them against independent data extracted from WORLDCLIM and SoilGrids at their native resolution of 0.0166°. If multiple vegetation plots fell into the same grid cell, we averaged

the plot-specific indicator values. We did the same for MCSE, which includes potential sampling biases, and compared the correlations with independent data (Extended Data Fig. 3). The analysis suggests that MCSE seems to be robust against potential sampling biases and rather benefits from the large amount of data available through crowd sensing. Overall, the MCSE approach underscores the potential of crowd-sensed plant occurrence data for large-scale environmental applications in line with previous studies on vegetation composition⁷⁵, biomes⁷⁶, phenology⁷⁷ and traits⁷⁸.

Statistical analysis of urban land-use–environment associations

We intersected the mapped climate and soil factors from MCSE for the city domains with CORINE land cover data (<https://land.copernicus.eu/en/products/corine-land-cover/clc2018> (ref. 63)). We considered the main urban land-use categories: 'Continuous urban fabric', 'Discontinuous urban fabric', 'Industrial and commercial units', 'Green urban areas', 'Forests' (combining 'Broad-leaved forest', 'Coniferous forest' and 'Mixed forest'), 'Arable land' (combining 'Non irrigated arable land', 'Permanently irrigated land' and 'Rice fields') and 'Pastures'.

For each environmental factor and city (c), we calculated an average value ($E^{u,c}$) from all grid cells within the specific land-use category (u) if at least 2.5% of the area specified by CORINE is covered by MCSE. We kept only cities for which $E^{u,c}$ could be calculated for all environmental factors and all considered urban land-use types. This yielded 326 cities across Europe with sufficient data availability. We further categorized the cities into five different regions: Nordic, British Isles, Eastern, Central and Southern (Extended Data Fig. 5), which correspond to different urban planning families⁷⁹ and geographic regions. This region classification provides a simple and clear stratification along latitudinal and longitudinal physiogeographic gradients and incorporates socioeconomic and historical–cultural differences relevant to urban systems.

To analyze general land-use–environment associations, we fitted mixed-effect analysis of variance models for each MCSE-based environmental factor ($E^{u,c}$). These models explain the environmental factors by the fixed effects of region (r), land-use class and their interaction, along with a random intercept for cities. To derive generalized patterns of land-use environment associations (Fig. 2) across cities, we calculated partial responses of environmental factors with respect to region and land use, integrating over the effect of city using the *emmeans* R package⁸⁰ (hereafter denoted as $M^{u,r}$; Supplementary Table 1 lists the marginal means, standard errors and 95% confidence intervals of the model parameters). For illustration, we present the region's effect as the deviation of the mean $M^{u,r}$ values per region from the overall mean of all $M^{u,r}$ values ($\Delta M^r = \text{mean}_u(M^{u,r}) - \text{mean}_{u,r}(M^{u,r})$; Fig. 2a). Furthermore, the effect of land-use type within each region is given as the deviation of $M^{u,r}$ per region and land-use class from the mean $M^{u,r}$ value per region ($\Delta M^{u,r} = M^{u,r} - \text{mean}_{u,r}(M^{u,r})$; Fig. 2b). For context, the analysis was repeated using a bioclimatic region classification⁸¹ instead of urban planning families⁷⁹—the results presented in Extended data Fig. 7 are qualitatively consistent with Fig. 2 and the conclusions remain unchanged.

Analysis of environmental differences within and between cities

To examine the environmental variation induced by urban land-use practices compared with large-scale geographic separations between cities (Fig. 3a), we compared environmental differences within cities ΔE_{within} to the environmental differences between cities $\Delta E_{\text{between}}$ based on their relative difference: $\Delta E_{\text{rel}} = \frac{\Delta E_{\text{between}} - \Delta E_{\text{within}}}{\Delta E_{\text{within}}}$. Thus, smaller environmental differences between cities compared with environmental differences within cities are reflected by negative relative differences, and indicate that urban land-use practices increased environmental gradients locally. We chose to analyze relative differences because they are comparable among different indicators showing different distributions—a corresponding analysis of absolute within-city versus

between-city gradients would yield identical conclusions but would require indicator-specific scales of the axes.

For each factor, the environmental difference within a city was determined by the maximum–minimum difference (amplitude) among land-use categories within a city: $\Delta E_{\text{within}}^c = \max_u(E^{u,c}) - \min_u(E^{u,c})$. We took the median value across cities to characterize the within-city environmental differences: $\Delta E_{\text{within}} = \text{median}_c(\Delta E_{\text{within}}^c)$. The environmental difference $\Delta E_{i,j}$ between two cities i and j is calculated as the absolute difference of values averaged over land-use types: $\Delta E_{i,j} = |\text{mean}_u(E^{u,c=i}) - \text{mean}_u(E^{u,c=j})|$. Similarly, the environmental difference of two cities for land-use type u is $\Delta E_{i,j}^u = |E^{u,c=i} - E^{u,c=j}|$. To account for spatial autocorrelation and to illustrate the distance decay of similarity³⁸, environmental differences between cities were stratified based on geographic distances between the cities within three distance classes d : 0–1,000 km, 1,000–2,000 km and >2,000 km (the largest distance is 3,225 km). Therefore, we calculated the median environmental difference across O_d , which denotes the set of all city pairs (i,j) that belong to distance class d : $\Delta E_{\text{between}}^d = \text{median}_{(i,j) \in O_d}(\Delta E_{(i,j)})$ for city means (Fig. 3a) and $\Delta E_{\text{between}}^{u,d} = \text{median}_{(i,j) \in O_d}(\Delta E_{(i,j)}^u)$ per land use (Fig. 3b). Considering urban forests as the most natural land-use type, a lower relative environmental difference and reduced distance decay of similarity (flatter slope) of another urban land-use type compared with forests indicate the homogenization of the respective land-use type among cities^{82,83}.

Data availability

Source data underlying Figs. 2 and 3 are provided with this paper. The gridded environmental datasets derived through MCSE including pan-European maps at 0.166° (~10 km) resolution, and high-resolution data for 326 European cities at 0.00166° (~100 m) are available via Zenodo (<https://zenodo.org/records/17733490>)⁸⁴. The used records of the crowd-sensed plant occurrence data across Europe are available from the GBIF (<https://www.gbif.org>) and include observations from Pl@ntNet (<https://www.plantnet.org>), iNaturalist (<https://www.inaturalist.org>), Observation.org (<https://observation.org>), Naturgucker.de (<https://www.naturgucker.de>), Artportalen (<https://www.artportalen.se>), the Norwegian Species Observation Service (Artsobservasjoner, <https://www.artsobservasjoner.no>), INPN—Inventaire National du Patrimoine Naturel (<https://inpn.mnhn.fr>), Arter.dk (<https://arter.dk>), FinBIF—the Finnish Biodiversity Information Facility (<https://laji.fi>) and iRecord (<https://www.brc.ac.uk/irecord>). Plant occurrence data from Flora Incognita (<https://floraincognita.com>) are not openly available due to data privacy protection and nature conservation policies, but can be made available for reproducibility purposes upon request to P.M. (patrick.maeder@tu-ilmenau.de). Used city boundaries are available from the Urban Audit (<https://ec.europa.eu/eurostat/web/cities>). CORINE land cover data are available at <https://land.copernicus.eu/pan-european/corine-land-cover>. Gridded mean annual temperature data from WorldClim v. 2.1 are available at <https://www.worldclim.org>. Gridded topsoil pH data from SoilGrids are available at <https://soilgrids.org>.

Code availability

All data analyses were performed in R (v. 4.1.2) using the following R packages: rgbif (v. 3.7.5), tidyverse (v. 2.0.0), ggplot2 (v. 3.5.1), data.table (v. 1.15.4), readxl (v. 1.4.3), terra (v. 1.7.39), tidyterra (v. 0.5.2), raster (v. 3.6.20), sf (v. 1.0.9), rnaturalearth (v. 0.3.2), giscoR (v. 0.4.0), ncd4 (v. 1.21), leaflet (v. 2.2.1), viridis (v. 0.6.3), scico (v. 1.5.0), emmeans (v. 1.8.9), lme4 (v. 1.1.35.3), patchwork (v. 1.2.0.9000) and geosphere (v. 1.5.18).

References

- IPCC. *Climate Change 2023: Synthesis Report. Contribution of Working Groups I, II and III to the Sixth Assessment Report of the Intergovernmental Panel on Climate Change* (2023).
- Oke, T. R. The energetic basis of the urban heat island. *Q. J. R. Meteorol. Soc.* **108**, 1–24 (1982).
- Brondizio, E. S., Settele, J., Díaz, S. & Ngo, H. T. *Global assessment report of the Intergovernmental Science-Policy Platform on Biodiversity and Ecosystem Services* (IPBES Secretariat, 2019).
- Zhang, X. et al. Urban drought challenge to 2030 sustainable development goals. *Sci. Total Environ.* **693**, 133536 (2019).
- Zhou, B., Rybski, D. & Kropp, J. P. The role of city size and urban form in the surface urban heat island. *Sci. Rep.* **7**, 13683 (2017).
- Li, Y., Schubert, S., Kropp, J. P. & Rybski, D. On the influence of density and morphology on the urban heat island intensity. *Nat. Commun.* **11**, 2647 (2020).
- Bowler, D. E., Buyung-Ali, L., Knight, T. M. & Pullin, A. S. Urban greening to cool towns and cities: a systematic review of the empirical evidence. *Landsc. Urban Plan.* **97**, 147–155 (2010).
- Zhou, W., Cao, W., Wu, T. & Zhang, T. The win-win interaction between integrated blue and green space on urban cooling. *Sci. Total Environ.* **863**, 160712 (2023).
- Milelli, M. et al. Characterization of the urban heat and dry island effects in the Turin metropolitan area. *Urban Clim.* **47**, 101397 (2023).
- Stolte, T. R. et al. Global drought risk in cities: present and future urban hotspots. *Environ. Res. Commun.* **5**, ad0210 (2023).
- Liu, J. & Niyogi, D. Meta-analysis of urbanization impact on rainfall modification. *Sci. Rep.* **9**, 7301 (2019).
- Van De Vijver, E., Delbecq, N., Verdoodt, A. & Seuntjens, P. Estimating the urban soil information gap using exhaustive land cover data: the example of Flanders, Belgium. *Geoderma* **372**, 114371 (2020).
- Shankar, M. et al. Unearthing the role of soils in urban climate resilience planning. *Nat. Sustain.* **7**, 1374–1376 (2024).
- Sukopp, H. & Starfinger, U. in *Ecosystems of the World* Vol. 16 (ed. Walker, L. R.) 397–412 (Elsevier, 1999).
- Morel, J. L., Chenu, C. & Lorenz, K. Ecosystem services provided by soils of urban, industrial, traffic, mining, and military areas (SUITMAS). *J. Soils Sediments* **15**, 1659–1666 (2015).
- De Kimpe, C. R. & Morel, J. L. Urban soil management: a growing concern. *Soil Sci.* **165**, 31–40 (2000).
- Li, Z.-G. et al. Soil nutrient assessment for urban ecosystems in Hubei, China. *PLoS ONE* **8**, 2–9 (2013).
- Greinert, A. The heterogeneity of urban soils in the light of their properties. *J. Soils Sediments* **15**, 1725–1737 (2015).
- Zhang, P. et al. Urban forest soil is becoming alkaline under rapid urbanization: a case study of Changchun, northeast China. *Catena* **224**, 106993 (2023).
- Lemoine-Rodriguez, R., Inostroza, L. & Zepp, H. The global homogenization of urban form. An assessment of 194 cities across time. *Landsc. Urban Plan.* **204**, 103949 (2020).
- Stuhlmacher, M. et al. Are global cities homogenizing? An assessment of urban form and heat island implications. *Cities* **126**, 103705 (2022).
- McKinney, M. L. Urbanization as a major cause of biotic homogenization. *Biol. Conserv.* **127**, 247–260 (2006).
- Aronson, M. F. J. et al. A global analysis of the impacts of urbanization on bird and plant diversity reveals key anthropogenic drivers. *Proc. R. Soc. B* **281**, 20133330 (2014).
- Groffman, P. M. et al. Ecological homogenization of urban USA. *Front. Ecol. Environ.* **12**, 74–81 (2014).
- Zonneveld, I. S. in *Ecological Indicators for the Assessment of the Quality of Air, Water, Soil, and Ecosystems* 207–217 (Springer, 1983).
- Diekmann, M. Species indicator values as an important tool in applied plant ecology—a review. *Basic Appl. Ecol.* **4**, 493–506 (2003).
- Dengler, J. et al. Ecological indicator values for Europe (EIVE) 1.0. *Veg. Classif. Surv.* **4**, 7–29 (2023).

28. Tichý, L. et al. Ellenberg-type indicator values for European vascular plant species. *J. Veg. Sci.* **34**, e13168 (2023).
29. Midolo, G. et al. Disturbance indicator values for European plants. *Glob. Ecol. Biogeogr.* **32**, 24–34 (2023).
30. Ellenberg, H. *Zeigerwerte der Gefäßpflanzen Mitteleuropas* 9th edn (Goltze, 1974).
31. Peng, S. et al. Surface urban heat island across 419 global big cities. *Environ. Sci. Technol.* **46**, 696–703 (2012).
32. Ackerman, B. Climatology of Chicago urban-rural differences in humidity. *J. Clim. Appl. Meteorol.* **26**, 427–430 (1987).
33. Huang, X. & Song, J. Urban moisture and dry islands: spatiotemporal variation patterns and mechanisms of urban air humidity changes across the globe. *Environ. Res. Lett.* **18**, 104010 (2023).
34. Meili, N., Paschalis, A., Manoli, G. & Fatichi, S. Diurnal and seasonal patterns of global urban dry islands. *Environ. Res. Lett.* **17**, 054012 (2022).
35. Slessarev, E. W. et al. Water balance creates a threshold in soil pH at the global scale. *Nature* **540**, 567–569 (2016).
36. O’Riordan, R., Davies, J., Stevens, C. & Quinton, J. N. The effects of sealing on urban soil carbon and nutrients. *Soil* **7**, 661–675 (2021).
37. Tobler, A. W. R. A computer movie simulating urban growth in the Detroit region. *Econ. Geogr.* **46**, 234–240 (1970).
38. Nekola, J. C. & White, P. S. The distance decay of similarity in biogeography and ecology. *J. Biogeogr.* **26**, 867–878 (2004).
39. Kühn, I., Brandl, R. & Klotz, S. The flora of German cities is naturally species rich. *Evol. Ecol. Res.* **6**, 749–764 (2004).
40. Delgado-Baquerizo, M. et al. Global homogenization of the structure and function in the soil microbiome of urban greenspaces. *Sci. Adv.* **7**, eabg5809 (2021).
41. Liu, X. et al. High-resolution multi-temporal mapping of global urban land using Landsat images based on the Google Earth Engine Platform. *Remote Sens. Environ.* **209**, 227–239 (2018).
42. Chen, G. et al. Global projections of future urban land expansion under shared socioeconomic pathways. *Nat. Commun.* **11**, 2302 (2020).
43. Güneralp, B., Reba, M., Hales, B. U., Wentz, E. A. & Seto, K. C. Trends in urban land expansion, density, and land transitions from 1970 to 2010: a global synthesis. *Environ. Res. Lett.* **15**, 044016 (2020).
44. Monrás-Janer, T. et al. Anthropogenic climate and land-use change drive short- and long-term biodiversity shifts across taxa. *Nat. Ecol. Evol.* **8**, 739–751 (2024).
45. Cardinale, B. J. et al. Biodiversity loss and its impact on humanity. *Nature* **486**, 59–67 (2012).
46. Heaviside, C., Macintyre, H. & Vardoulakis, S. The urban heat island: implications for health in a changing environment. *Curr. Environ. Health Rep.* **4**, 296–305 (2017).
47. Bratman, G. N. et al. Nature and mental health: an ecosystem service perspective. *Sci. Adv.* **5**, eaax0903 (2019).
48. Hammoud, R. et al. Smartphone-based ecological momentary assessment reveals an incremental association between natural diversity and mental wellbeing. *Sci. Rep.* **14**, 7051 (2024).
49. Mäder, P. et al. The Flora Incognita app—interactive plant species identification. *Methods Ecol. Evol.* **12**, 1335–1342 (2021).
50. Affouard, A. et al. Pl@ntNet automatically identified occurrences. *GBIF* <https://doi.org/10.15468/mma2ec> (2023).
51. Affouard, A. et al. Pl@ntNet observations. *GBIF* <https://doi.org/10.15468/gtebaa> (2023).
52. iNaturalist contributors. iNaturalist research-grade observations. *GBIF* <https://doi.org/10.15468/ab3s5x> (2024).
53. Observation.org. Observation.org, nature data from around the world. *GBIF* <https://doi.org/10.15468/5nilie> (2024).
54. Naturgucker.de. Naturgucker.de NABU|naturgucker. *GBIF* <https://doi.org/10.15468/uc1apo> (2024).
55. SLU Artdatabanken. Artportalen. Version 92.403. *GBIF* <https://doi.org/10.15468/killkyl> (2024).
56. The Norwegian Biodiversity Information Centre & Hoem, S. Norwegian Species Observation Service. Version 1.298. *GBIF* <https://doi.org/10.15468/zjbzel> (2024).
57. Inventaire National du Patrimoine Naturel (INPN). Application INPN Espèces: observations naturalistes, participatives et opportunistes, fondées sur des photographies. Version 1.1. *GBIF* <https://doi.org/10.15468/2wgzwe> (2022).
58. Arter Project Group. Species recordings from the Danish National Portal Arter.dk. *GBIF* <https://doi.org/10.15468/q3yy4u> (2020).
59. Finnish Biodiversity Information Facility. Lajitietokeskus/FinBIF—Notebook, general observations. *GBIF* <https://doi.org/10.15468/4g56tp> (2024).
60. Botanical Society of Britain & Ireland. Vascular plant records verified via iRecord. *GBIF* <https://doi.org/10.15468/s4bje6> (2024).
61. Natural England. iRecord surveys. *GBIF* <https://doi.org/10.15468/i7x5ca> (2024).
62. Chamberlain, S. et al. rgbif: interface to the global biodiversity information facility API. *CRAN* <https://cran.r-project.org/package=rgbif> (2024).
63. European Environment Agency. *EEA Geospatial Data Catalogue CORINE Land Cover 2018 (raster 100 m), Europe, 6-yearly* (2020).
64. Hernangómez, D. giscoR: Download Map Data from GISCO API—Eurostat. *Zenodo* <https://doi.org/10.5281/zenodo.4317946> (2024).
65. Fick, S. E. & Hijmans, R. J. WorldClim 2: new 1-km spatial resolution climate surfaces for global land areas. *Int. J. Climatol.* **37**, 4302–4315 (2017).
66. Poggio, L. et al. SoilGrids 2.0: producing soil information for the globe with quantified spatial uncertainty. *Soil* **7**, 217–240 (2021).
67. Nussbaum, M., Zimmermann, S., Walthert, L. & Baltensweiler, A. Benefits of hierarchical predictions for digital soil mapping—an approach to map bimodal soil pH. *Geoderma* **437**, 116579 (2023).
68. Scherrer, D., Massy, S., Meier, S., Vittoz, P. & Guisan, A. Assessing and predicting shifts in mountain forest composition across 25 years of climate change. *Divers. Distrib.* **23**, 517 (2017).
69. Tautenhahn, S. et al. On the biogeography of seed mass in Germany—distribution patterns and environmental correlates. *Ecography* **31**, 457–468 (2008).
70. Descombes, P. et al. Spatial modelling of ecological indicator values improves predictions of plant distributions in complex landscapes. *Ecography* **43**, 1448–1463 (2020).
71. Scherrer, D. & Guisan, A. Ecological indicator values reveal missing predictors of species distributions. *Sci. Rep.* **9**, 3064 (2019).
72. Knapp, S., Kühn, I., Stolle, J. & Klotz, S. Changes in the functional composition of a Central European urban flora over three centuries. *Perspect. Plant Ecol. Evol. Syst.* **12**, 235–244 (2010).
73. Ostrowski, G., Aicher, S., Mankiewicz, A., Chusova, O. & Dembic, I. Mean ecological indicator values: use EIVE but no cover-weighting. *Veg. Classif. Surv.* **6**, 57–67 (2025).
74. Sabatini, F. M. et al. sPlotOpen—an environmentally balanced, open-access, global dataset of vegetation plots. *Glob. Ecol. Biogeogr.* **30**, 1740–1764 (2021).
75. Botella, C., Joly, A., Bonnet, P., Munoz, F. & Monestiez, P. Jointly estimating spatial sampling effort and habitat suitability for multiple species from opportunistic presence-only data. *Methods Ecol. Evol.* **12**, 933–945 (2021).
76. Scheiter, S., Wolf, S. & Kattenborn, T. Crowd-sourced trait data can be used to delimit global biomes. *Biogeosciences* **21**, 4909–4926 (2024).
77. Rzanny, M., Mäder, P., Wittich, H. C., Boho, D. & Wäldchen, J. Opportunistic plant observations reveal spatial and temporal gradients in phenology. *npj Biodivers.* **3**, 5 (2024).

78. Wolf, S. et al. Citizen science plant observations encode global trait patterns. *Nat. Ecol. Evol.* **6**, 1904 (2022).
79. Davies, C. et al. *Green Infrastructure Planning and Implementation: the Status of European Green Space Planning and Implementation based on an Analysis of Selected European City-Regions* (Green Surge Report, 2015).
80. Searle, S. R., Speed, F. M. & Milliken, G. A. Population marginal means in the linear model: an alternative to least squares means. *Am. Stat.* **34**, 216–221 (1980).
81. Condé, S. & Richard, D. *Europe's Biodiversity—Biogeographical Regions and Seas. Biogeographical Regions in Europe: Introduction* (European Environment Agency, 2002).
82. Decker, O. et al. Distance decay reveals contrasting effects of land-use types on arthropod community homogenization. Preprint at *Res. Sq.* <https://doi.org/10.21203/rs.3.rs-4522164/v1> (2024).
83. Lokatis, S. & Jeschke, J. M. Urban biotic homogenization: approaches and knowledge gaps. *Ecol. Appl.* **32**, eap.2703 (2022).
84. Tautenhahn, S. Mobile crowd sensing of environments (MCSE): ecological indicator value maps from citizen-science plant observations for Europe and European cities. *Zenodo* <https://doi.org/10.5281/zenodo.17733490> (2025).
85. Kopecký, M., Hederová, L., Macek, M., Klinerová, T. & Wild, J. Forest plant indicator values for moisture reflect atmospheric vapour pressure deficit rather than soil water content. *New Phytol.* **244**, 2109–2123 (2024).
86. Schaffers, A. P. & Sýkora, K. V. Reliability of Ellenberg indicator values for moisture, nitrogen and soil reaction: a comparison with field measurements. *J. Veg. Sci.* **11**, 225–244 (2000).
- from U.W., M. Rzanny, B.A. and J.W., whereas the Flora Incognita data were provided by P.M., J.W., M. Rzanny, H.C.W. and D.B. S.T. performed the statistical analysis with input from M.J., J.W., M. Reichstein, M. Rzanny, U.W. and B.A. Interpretation and discussion of the results were supported by J.W., M. Rzanny, M. Reichstein, G.M., M.C., J.D., F.J. and L.T. S.W., A.B. and N.K. improved clarity and presentation. J.W. and P.M. acquired funding. All authors reviewed and approved the final version.

Funding

Open access funding provided by Max Planck Society.

Competing interests

The authors declare no competing interests.

Additional information

Extended data is available for this paper at <https://doi.org/10.1038/s44284-025-00378-9>.

Supplementary information The online version contains supplementary material available at <https://doi.org/10.1038/s44284-025-00378-9>.

Correspondence and requests for materials should be addressed to Susanne Tautenhahn.

Peer review information *Nature Cities* thanks Karen De Pauw, David Rossiter and Stefan Klotz for their contribution to the peer review of this work.

Reprints and permissions information is available at www.nature.com/reprints.

Publisher's note Springer Nature remains neutral with regard to jurisdictional claims in published maps and institutional affiliations.

Open Access This article is licensed under a Creative Commons Attribution 4.0 International License, which permits use, sharing, adaptation, distribution and reproduction in any medium or format, as long as you give appropriate credit to the original author(s) and the source, provide a link to the Creative Commons licence, and indicate if changes were made. The images or other third party material in this article are included in the article's Creative Commons licence, unless indicated otherwise in a credit line to the material. If material is not included in the article's Creative Commons licence and your intended use is not permitted by statutory regulation or exceeds the permitted use, you will need to obtain permission directly from the copyright holder. To view a copy of this licence, visit <http://creativecommons.org/licenses/by/4.0/>.

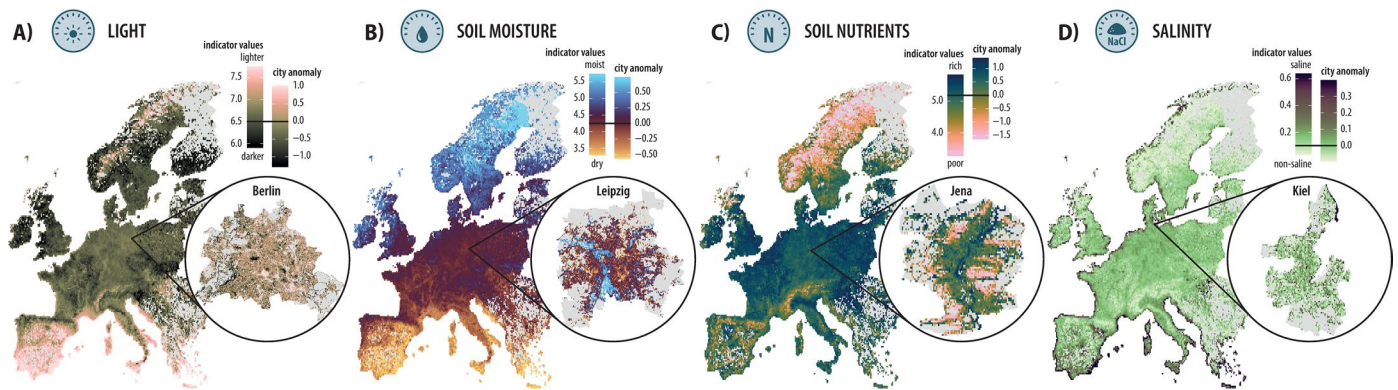
© The Author(s) 2026

Acknowledgements

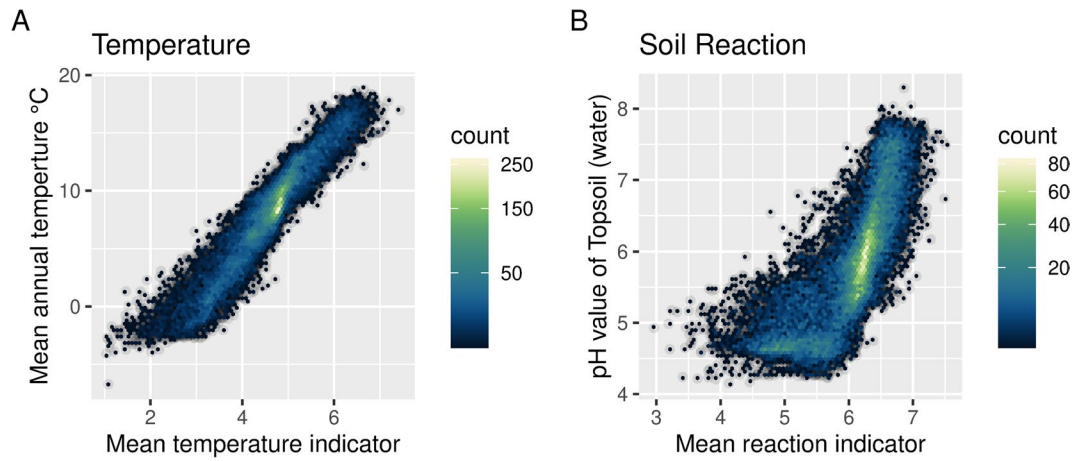
We thank the millions of plant observers for making this work possible through their curiosity. G. Blougouras contributed to discussions on urban ecology. A. Börner designed Fig. 1 and Extended Data Fig. 1. R. Kiese, H. Imhof, F. Schneider and A. Frick provided expertise on the availability of independent environmental data and evaluation. This study was funded by the Federal Agency for Nature Conservation (BfN) and the National Monitoring Center for Biodiversity, with funds from the German Federal Ministry for the Environment, Nature Conservation, Building and Nuclear Safety (BMUB) grant number 352460010A (H.C.W. and D.B.) and 352460010B (S.T. and A.B.); the German Federal Ministry of Education and Research grant numbers 16LC2019A1 (P.M.) and 16LC2019B1 (J.W.), the Carl Zeiss Foundation grant number P2022-08-006 (M. Rzanny) and the Horizon Europe project AI4SoilHealth grant number 101086179 (B.A.). This article was published under the Max Planck Society's Nature Read and Publish agreement (2025–2028), covering the OA fees.

Author contributions

S.T. and M.J. conceived the study and drafted the manuscript. S.T. derived and evaluated the grid-based MCSE data with contributions

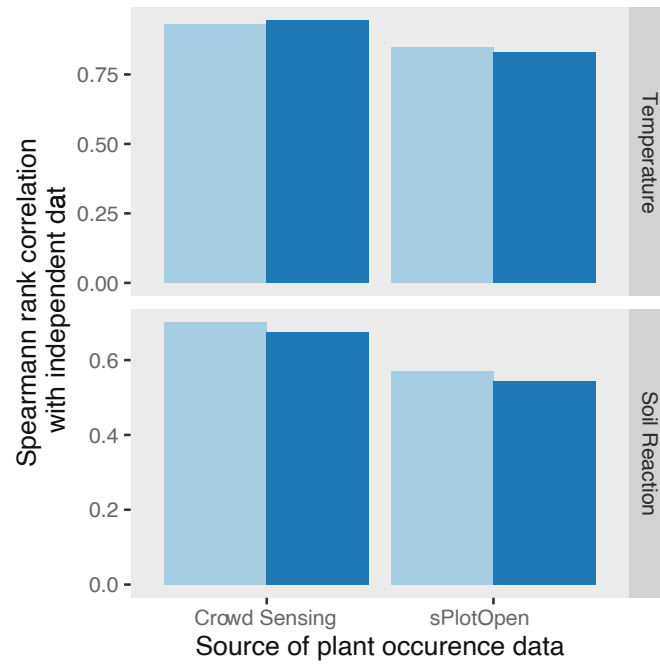


Extended Data Fig. 1 | MCSE-derived maps for the European domain and selected cities. a–d, MCSE-derived maps for light (a), soil moisture (b), soil nutrients (c) and salinity (d) for the European domain, and for selected cities. Please note the different color scales for the European and city domains.



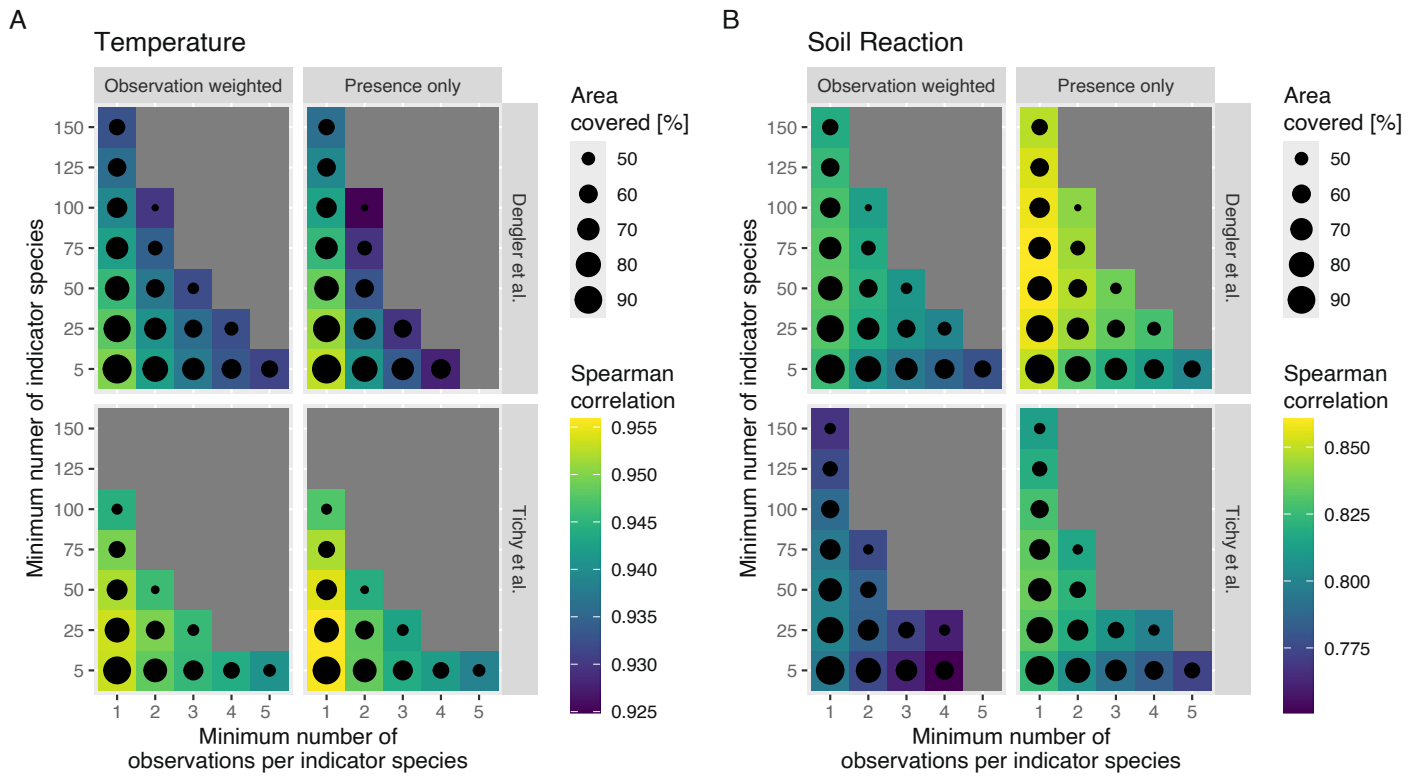
Extended Data Fig. 2 | Corroboration of MCSE with independent data products over Europe. Comparison of the temperature from MCSE with mean annual temperature from WORLDCLIM (A; $\text{cor} = 0.96$), and comparison of the soil reaction from MCSE with top soil pH from SoilGrids (B; $\text{cor} = 0.86$).

Correspondence is quantified with Spearman rank correlation coefficient. The apparent non-linear relationship for soil pH deteriorates the correlation and is likely an artifact of the SoilGrids product, which shows little variations below a pH value of 5.



Extended Data Fig. 3 | Corroboration of MCSE with citizen science and expert based vegetation data. Parallel evaluation of the correlation of indicator values calculated from 40,000 expert-based vegetation plots (sPlotOpen) vs calculated from crowd-sensed plant occurrences used by MCSE at the same locations with

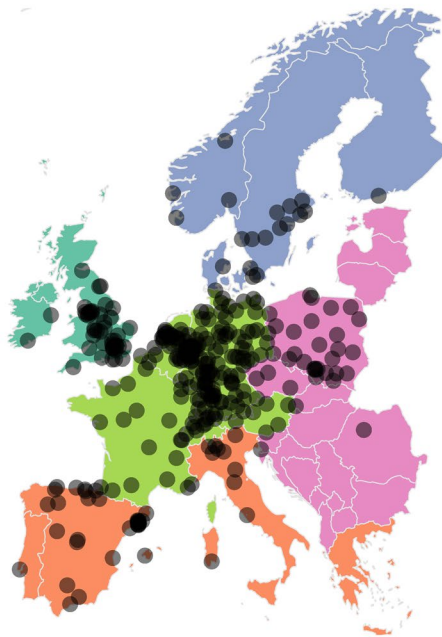
independent data of temperature and soil pH (see also Extended Data Fig. 2). The corroboration supports the usage of crowd-sensed plant occurrence data to calculate indicator values from both indicator value systems.



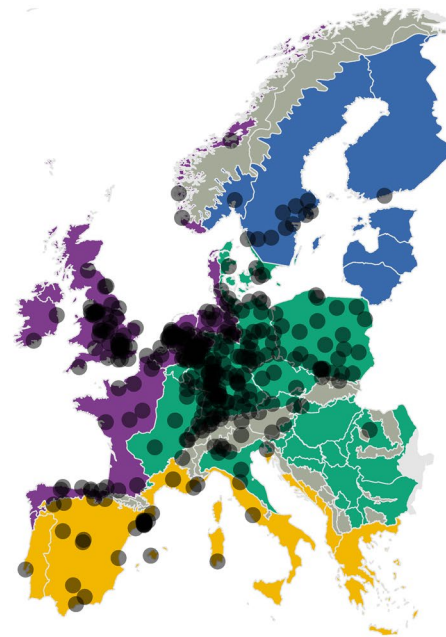
Extended Data Fig. 4 | Results from full-factorial sensitivity analysis of methodological choices of Mobile-Crowd-Sensing of Environment (MCSE). **A:** Results for MCSE derived temperature based on comparison with mean annual temperature from WORLDCLIM. **B:** Results for MCSE derived soil reaction

based on comparison with top-soil pH from SoilGrids. Area covered indicates the fraction of the European domain that could be mapped by MCSE with these settings. The narrow range of variation in correlation reflects strong robustness to settings in general.

Assigning cities to regions

A
Planning families

■ Nordic	■ British isles
■ Eastern	■ Central
■ Southern	

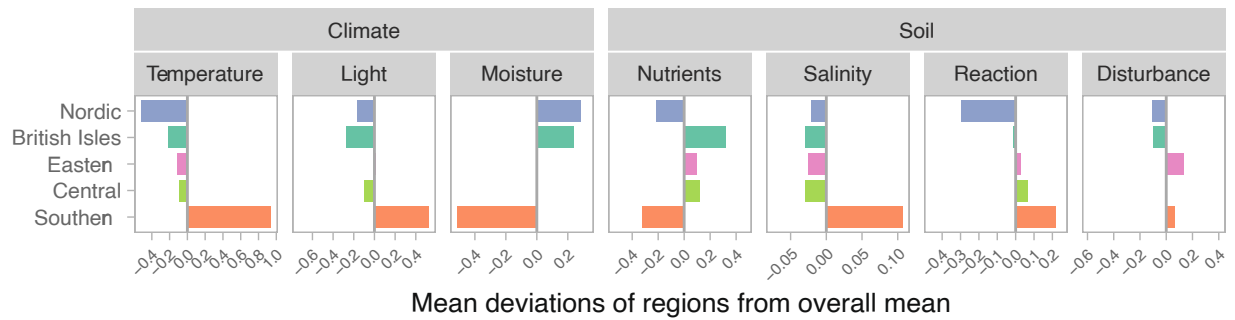
B
Biogeographic regions

■ Mediterranean	■ Continental-Pannonian
■ Atlantic	■ Boreal
■ Alpine	■ NA

Extended Data Fig. 5 | Map of the 326 cities used in the study, and associated regions. The division of cities into regions was done **A**) by using planning families⁵¹ representing political differences and planning traditions (applied in Fig. 2) and Extended Data Fig. 6) and **B**) by using biogeographic regions⁵³ (applied in Extended Data Fig. 7).

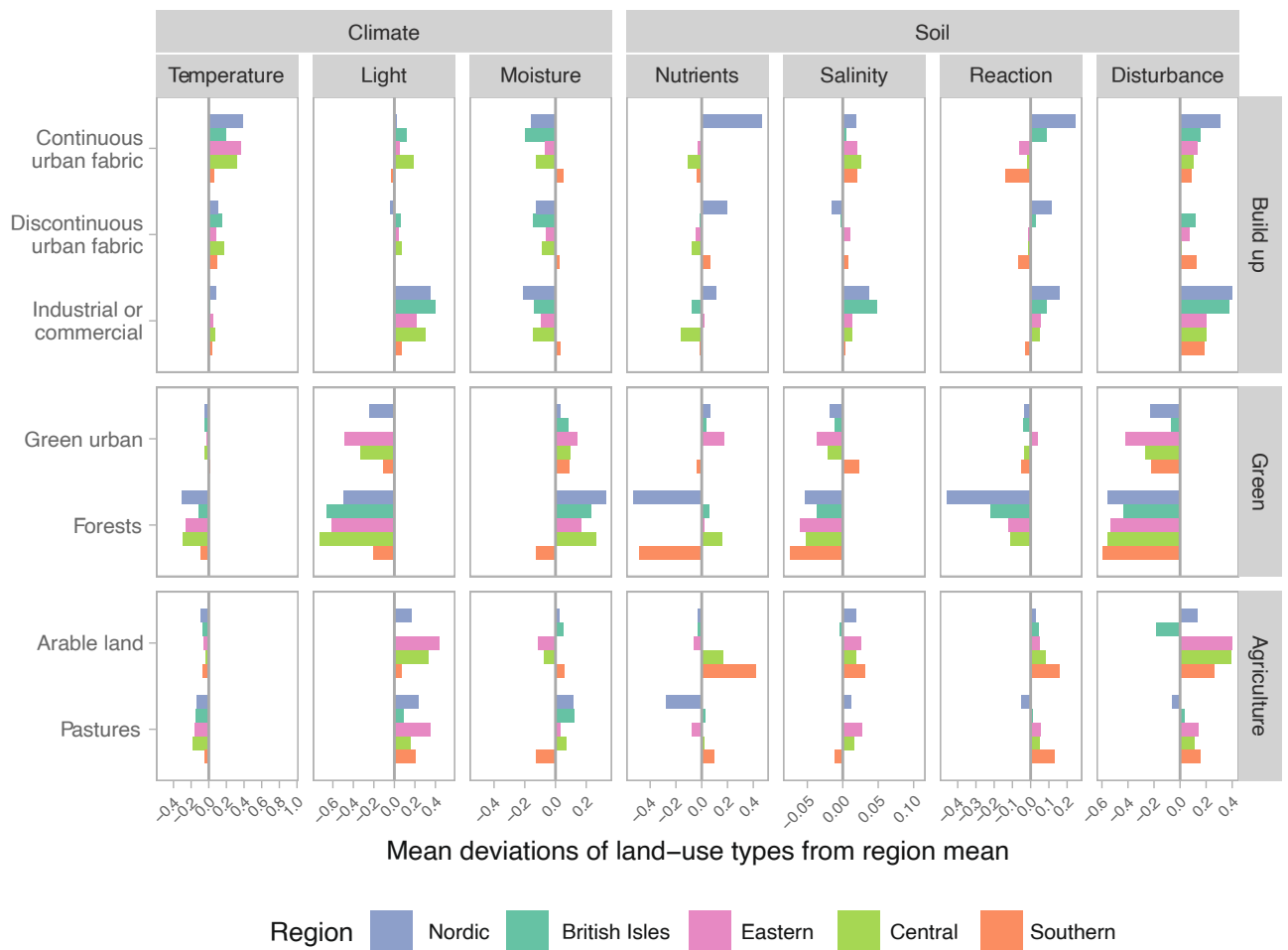
A

Large scale geographic variations of urban environments



B

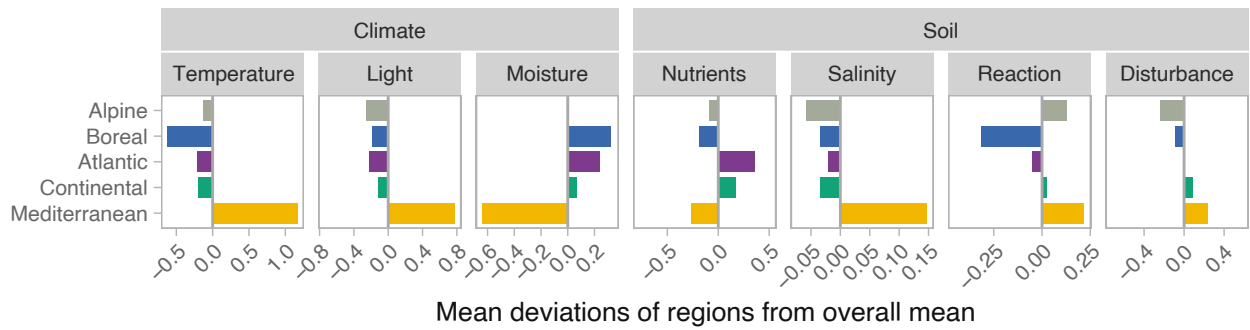
Small scale land-use specific variations of urban environments



Extended Data Fig. 6 | Extended version of Fig. 2. Extended version of Fig. 2 including light and nutrients conditions as well as agricultural land-use classes (Arable land, Pastures). See Supporting data table of Fig. 1 for marginal means (EMMs), standard errors, and 95% confidence intervals of model parameters.

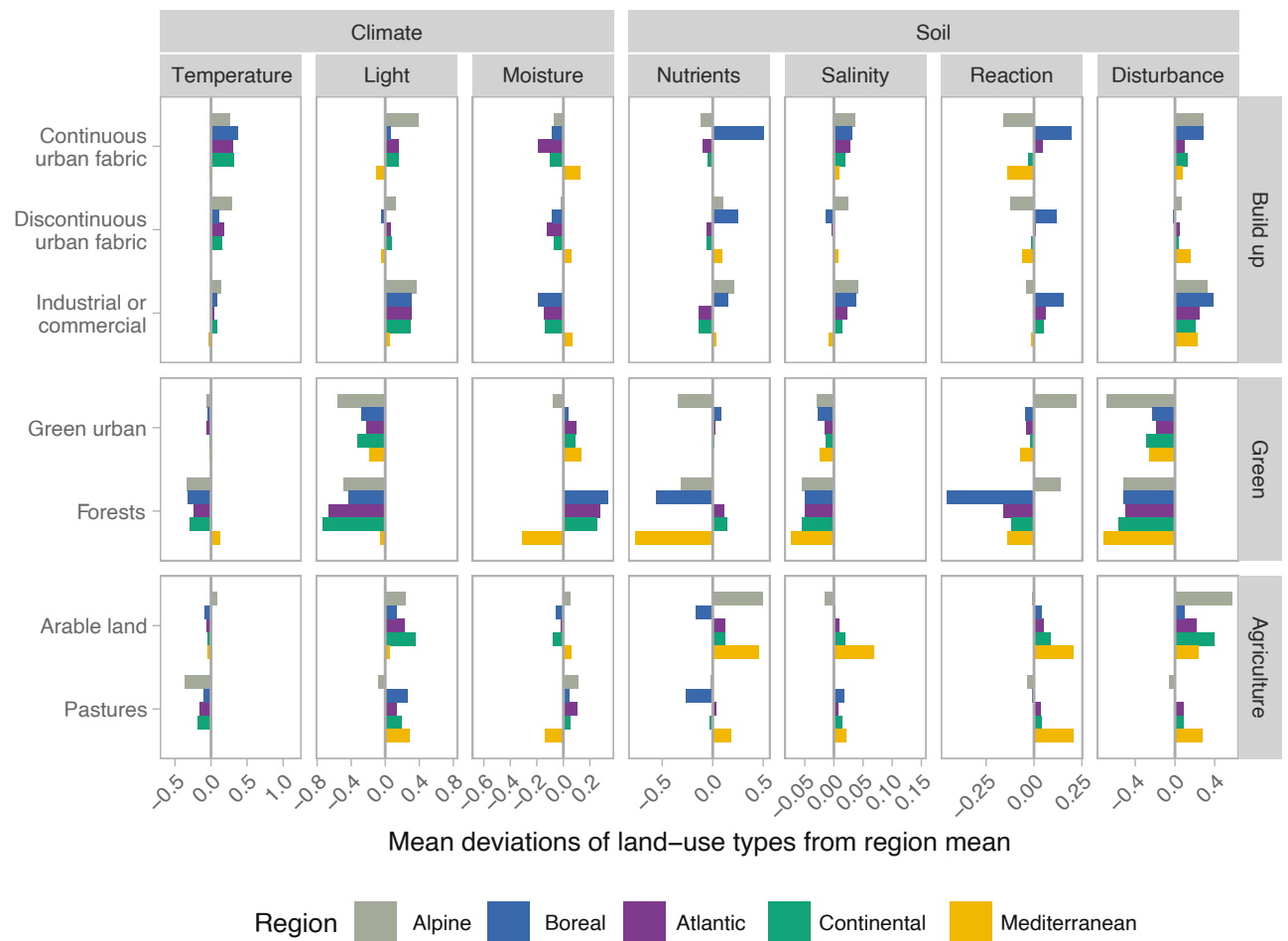
A

Large scale biogeographic variations of urban environments



B

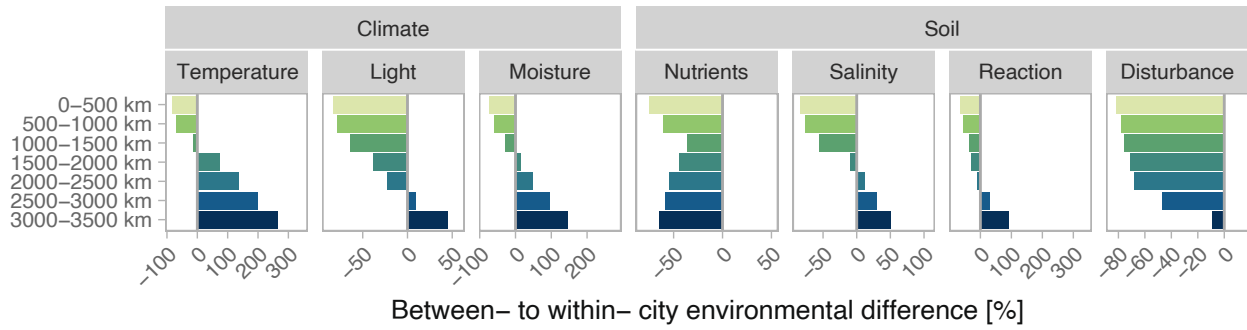
Small scale land-use specific variations of urban environments



Extended Data Fig. 7 | Version of Fig. 2 based on biogeographic regions instead of planning families. Same as Extended data Fig. 6 but based on the EEA Biogeographic regions^{S3} instead of planning families^{S1} for the separation of regions.

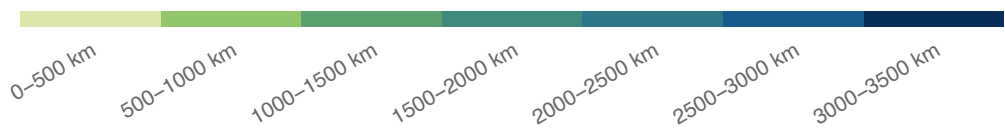
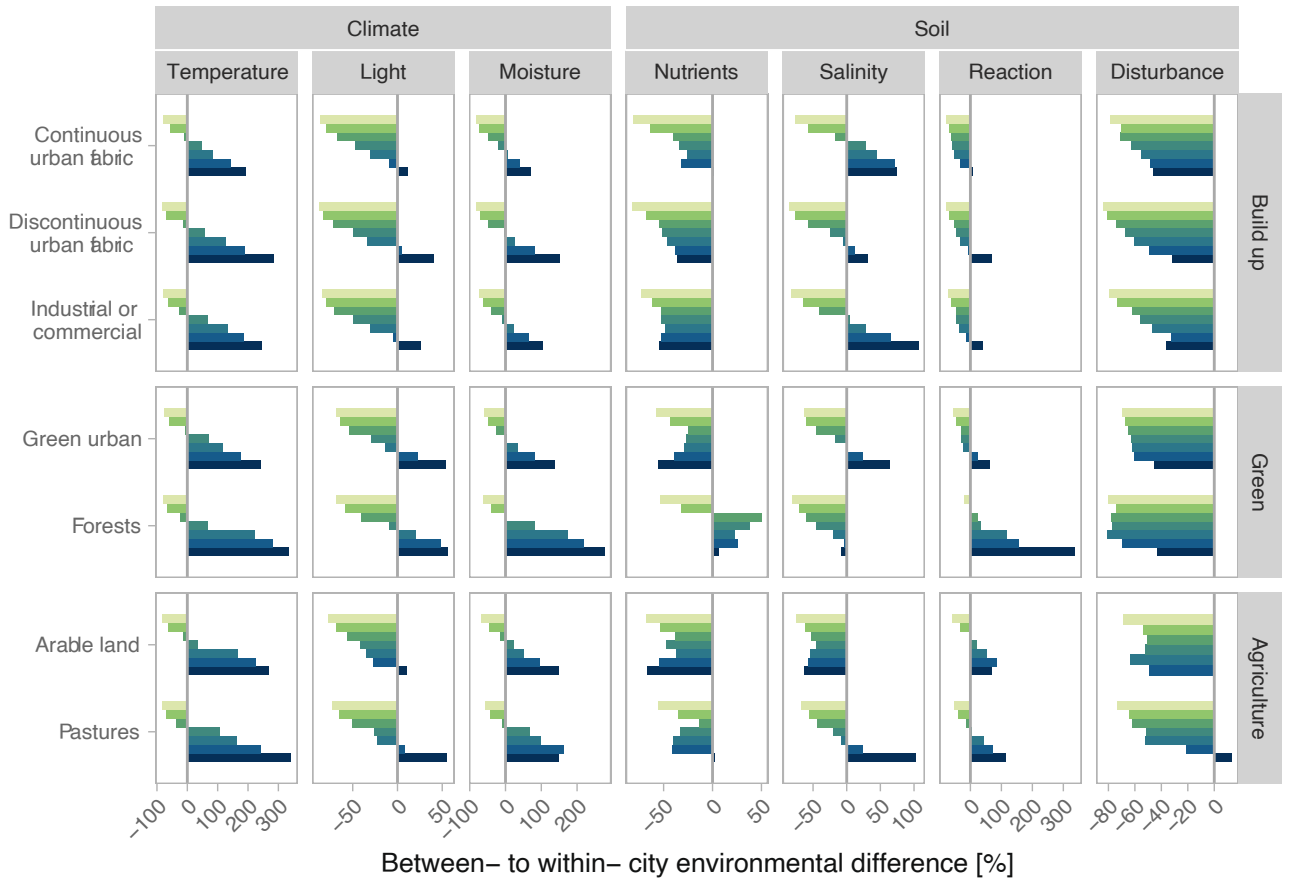
A

City mean environmental differences by geographic distance



B

Land-use specific environmental differences by geographic distance



Extended Data Fig. 8 | Extended version of Fig. 3. Extended version of Fig. 3 including light and nutrients conditions as well as agricultural land-use classes (Arable land, Pastures).